Invited Paper

MRA Based Wavelet Frames and Applications: Image Segmentation and Surface Reconstruction

Bin Dong[1] and Zuowei Shen[2]

[1] Department of Mathematics, The University of Arizona, 617 N Santa Rita Ave, Tucson, AZ, USA, 85721-0089

[2] Department of Mathematics, National University of Singapore, Block S17, 10 Lower Kent Ridge Road, Singapore, 119076

ABSTRACT

Theory of wavelet frames and their applications to image restoration problems have been extensively studied for the past two decades. The success of wavelet frames in solving image restoration problems, which includes denoising, deblurring, inpainting, computed tomography, etc., is mainly due to their capability of sparsely approximating piecewise smooth functions such as images. However, in contrast to the wide applications of wavelet frame based approaches to image restoration problems, they are rarely used for some image/data analysis tasks, such as image segmentation, registration and surface reconstruction from unorganized point clouds. The main reason for this is the lack of geometric interpretations of wavelet frames and their associated transforms. Recently, geometric meanings of wavelet frames have been discovered and connections between the wavelet frame based approach and the differential operator based variational model were established.[1] Such discovery enabled us to extend the wavelet frame based approach to some image/data analysis tasks that have not yet been studied before. In this paper, we will provide a unified survey of the wavelet frame based models for image segmentation[2] and surface reconstruction from unorganized point clouds.[3] Advantages of the wavelet frame based approach are illustrated by numerical experiments.

Keywords: Image segmentation, surface reconstruction, variational method, (tight) wavelet frames, split Bregman algorithm.

1. INTRODUCTION

1.1 Wavelet Frames and Applications in Image Restoration

The theory of the multiresolution analysis (MRA) based wavelet frames, especially tight wavelet frames, were extensively studied in the past two decades.[4–8] Examples of tight frames includes translation invariant wavelets,[9] curvelets,[10] and framelets,[5] etc. In contrast to orthogonal bases, tight frames provide redundant representations to signals and images. The redundancy of tight frames usually gives more robust algorithms and the wavelet system leads to sparse approximation for piecewise smooth functions, such as images, due to their short supports and high orders of vanishing moments. Such property is known to be desirable for image restoration problems including denoising, inpainting, deblurring, and medical imaging (e.g. CT and MRI).

Image restoration problems can be generally classified as ill-posed linear inverse problems. If the problem is not carefully handled, the solution one obtains may contain various artifacts due to the ill-pose nature of the problem. In order to reduce the amount of artifacts while preserving key features of the image, e.g. edges, various regularization based optimization models were proposed in the literature. Among all regularization based models for image restoration, variational methods and wavelet frames based approaches are widely adopted and have been proven successful. The trend of variational methods for image restoration started with the refined Rudin-Osher-Fatemi (ROF) model[11] which penalizes the total variation (TV) of the image to be recovered. The ROF model is especially effective on restoring images that are piecewise constant, e.g., binary images. Other

(Send correspondence to Zuowei Shen)
Bin Dong: E-mail: dongbin@math.arizona.edu
Zuowei Shen: E-mail: matzuows@nus.edu.sg

Independent Component Analyses, Compressive Sampling, Wavelets, Neural Net, Biosystems, and Nanoengineering X, edited by Harold Szu, Liyi Dai, Proc. of SPIE Vol. 8401, 840102 · © 2012 SPIE · CCC code: 0277-786X/12/$18
doi: 10.1117/12.923203

types of variational models were also proposed after the ROF model. We refer the interested readers to the papers[12–19] and the references therein for further details.

Wavelet frame based approaches for image restoration are relatively new and came from a different path. The basic idea of wavelet frame based approaches is that images can be sparsely approximated by properly designed wavelet frames, and hence, the regularization used for the majority of wavelet frame based models is the ℓ_1-norm of the wavelet frame coefficients. Due to redundancy of wavelet frames, there are three different formulations of wavelet frame based models: the analysis based approach,[20,21] the synthesis based approach[22–26] and the balanced approach.[27,28] Wavelet frame based approaches were further developed and applied for general image restoration problems[27–36] and medical imaging.[37,38] More recently, the property of sparse approximation of wavelet frames was further explored for image restoration problems, where the ℓ_0-norm of the wavelet frame coefficients was penalized instead of the ℓ_1-norm.[39,40]

Although wavelet frame based approaches have been well developed and widely adopted in image restoration, their applications to some image/data analysis tasks are rarely known, especially those requiring geometric regularization of the objects-of-interest in the images/data, such as image segmentation, image registrations, surface reconstruction from unorganized point clouds, etc. In the literature, such problems can be well described and solved by variational models instead.

The main obstacle of extending wavelet frame based approaches to tackle such problems was the lack of geometric interpretation of wavelet frame transforms and wavelet frame based models. Since variational models are widely used to solve those problems, it is natural to study the relations between wavelet frame based models and variational models. In image restoration, although wavelet frame based models take similar forms as variational models, they were generally considered as different approaches because, among many other reasons, wavelet frame based approaches is defined for discrete data, while variational methods assume all variables are functions. In addition, the theoretical development of wavelet frames is different in flavor from that of variational techniques. Although some studies in the literature indicated that there was a relation between Haar wavelet and total variation,[41] it was unclear if there exists a general relation between wavelet frames and variational models (with general differential operators). This fundamental question was recently answered by Cai et al.[1] where the authors established a general connection between one of the wavelet frame based approaches, namely the analysis based approach, and a general variational model. It was shown that the analysis based approach can be regarded as a finite difference approximation of a general variational model with a general differential operator; and different choices of parameters, as well as wavelet frames, of the analysis based approach result in different orders of approximation as image resolution goes to infinity. More interestingly, through a careful analysis the authors showed that the solutions (i.e. minimizers or approximate minimizers) of the analysis based approach also approximate the solutions of the corresponding variational model. Such connections not only grant geometric interpretation to wavelet frame transform and wavelet frame based models, but also enable us to extend the application of wavelet frames to other image and data analysis tasks including image segmentation[2] and surface reconstruction.[3]

In this paper, we focus on a survey of the recent developments of the applications of wavelet frames in image segmentation[2] and surface reconstruction from unorganized point clouds.[3]

1.2 Image Segmentation

Image segmentation is an important problem in computer vision and medical image analysis. The objective of image segmentation is to provide a visually meaningful partition of the image domain. Although it is usually an easy task for human to separate background and different objects for a given image, it is still a great challenge to design automated algorithms for image segmentation in general.[15,18,42]

Image segmentation can be formulated mathematically as follows. Given an image f and its domain Ω, based on its gray values (or RGB values for color images), we seek a "meaningful" partition of Ω as follows:

$$\Omega = \Omega_1 \cup \Omega_2 \cup \cdots \cup \Omega_m.$$

Here, Ω_1 is the background of the image f and Ω_j, $j = 2, \ldots, m$, are the domains representing different objects-of-interest. In this paper, we will focus on the particular case $m = 2$, i.e. the two-phases image segmentation

problem. One of the main challenge for image segmentation is that a "meaningful" partition is not only image dependent, but also application dependent. In other words, if the target image f is changed, or, for the same image f, the ultimate objective of image segmentation is changed, one should obtain a different partition of the domain Ω. Therefore, it is an art to design a partitioning rule according to the specific type of image and application in hand.

Regularization based variational techniques have been widely used for general image segmentation problems. It is rather crucial to incorporate any prior knowledge one may have for the domains of the objects-of-interest Ω_j or their boundaries $\partial\Omega_j$. Variational image segmentation started with the work by Mumford and Shah[42] and the active contour models.[43–45] Based one the Mumford-Shah formulation and level set method, the Chan-Vese model[46,47] (also known as active contour without edges, i.e. ACWE) was proposed which improves the earlier results in terms of both segmentation accuracy and computation efficiency. In the later work,[48,49] the authors proposed a segmentation model by replacing the regularization term of the Chan-Vese model by the geometric active contour functional,[44] which generates better segmentation results. More recently, convexified models[50–53] for the Chan-Vese model, as well as the improved model of Chan-Vese,[48] were proposed which significantly improved computation efficiency for general image segmentation problems. When more specific knowledge of the objects-of-interest is available, properly designed shape priors can be used instead of generic priors.[54–56]

Other than variational models, wavelets and wavelet frames were also applied to texture classification and segmentation.[57,58] However, it was not clear how we could apply wavelet frames to general image segmentation tasks and what was their relation to variational techniques. This question was recently answered by Dong, Chien and Shen,[2] where they proposed a general wavelet frame based two-phases image segmentation model.

Image segmentation plays an important role in medical image analysis as well. Segmenting biological structures, e.g. cortical or subcortical structures, blood vessels, tumors etc., from various types of medical images is very important for detecting abnormalities, studying and tracking progress of diseases, and surgery planning. Medical image segmentation is a difficult problem due to the fact that medical images commonly have poor contrasts, different types of noise, and missing or diffuse boundaries. There are numerous algorithms developed in the literature targeting on the segmentation of biological structures. We refer interested readers to the papers[59–68] and the references therein for further details.

1.3 Surface Reconstruction

Surface reconstruction from unorganized/scattered point clouds (shall be called surface reconstruction in short), is an important problem in geometric modeling. Given a set of scattered points

$$\boldsymbol{X} = \{x_1, x_2, \ldots, x_n\} \subset \Omega \subset \mathbb{R}^3$$

that are sampled from some unknown surface $\mathcal{S}$, the surface reconstruction problem is to construct a surface $\widehat{\mathcal{S}}$ from the observed data $\boldsymbol{X}$ such that $\widehat{\mathcal{S}}$ approximates $\mathcal{S}$. It has received a lot of attention in the computer graphics community in recent years because of the fast development of laser scanner technology which enables the point-based representation for highly detailed surfaces, and its wide applications in areas such as reverse engineering, product design, medical appliance design, archeology, etc.

Surface reconstruction has been studied for decades and has a rich literature. One of the earliest algorithm was to locally estimated the signed distance function of the true surface based on the measured point samples.[69] Smooth surfaces can also be built by fitting radial basis functions to a given point cloud,[70] which was later adapted to large data sets.[71] A variational level set method was later proposed by Zhao et al.[72] where an energy functional was introduced that utilized the distance function associated to the given data points; and the energy functional was minimized by solving a level set equation derived from the gradient flow. More recently, extensions of the earlier work of Zhao et al.[72] were proposed[73–75] where computation efficiency of surface reconstruction was greatly improved.

Rather than computing a single global approximation for a given point cloud, the approaches utilizing the moving least squares locally fit smooth functions to each subset of sampled points and then smoothly combine the fitting functions together.[76,77] A different and yet related approach is known as the nonlinear projection method.[78] A point-set surface is defined as the set of stationary points of a projection operator, which was first

used for point based modeling and rendering.[79] Another popular approach is to construct a polyhedral surface from the input set of points using the Voronoi diagram,[80–84] which is closely related to Voronoi-based algorithms for medial axis estimation.

When the given set of points are sampled from the graph of a 2-dimensional function, a wavelet frame based model was proposed by Ji et al.,[85] where the authors used a simple principal shift invariant space and its associated wavelet frame transform to fit the given data points. However, the assumption that the points are sampled from a graph of a function is not satisfied for certain applications, such as the data obtained from a 3D laser scanner. The first wavelet frame based model that reconstructs surfaces from general scattered points was recently proposed by Dong and Shen.[3]

2. WAVELET FRAME BASED APPROACHES

Image segmentation and surface reconstruction are generally considered as different problems in the literature. Indeed, image segmentation is to determine a certain meaningful partition of the image domain based on image intensities, while surface reconstruction is to determine a surface that interpolates or approximates the given sample points. However, the development of level set method for image segmentation and surface reconstruction has somehow unified the two different problems. The basic idea is to find a level set function whose 0 level set (or in general, γ level set) labels the boundary of the object-of-interest for image segmentation; or represents the reconstructed surface for surface reconstruction.

We start this section by a brief introduction of wavelet frames. Then, we will present a general wavelet frame based model, together with a fast numerical algorithm, for both image segmentation and surface reconstruction. The wavelet frame based model can be regarded as certain discretization of a general variational model using general differential operators.[1–3] However, using wavelet frame based formulation has clear advantages over standard discretization of the variational model, as what has already been discovered in image restoration.[27, 36–38] First of all, fast wavelet frame based optimization algorithms used for image restoration problems can also be applied for image segmentation and surface reconstruction. Secondly, the wavelet frame transforms contains a rich family of difference operators that can be understood as various discretizations of a family of differential operators. The multi-level nature of the wavelet frame decomposition automatically applies different difference operators adaptively to the geometric structure of the level sets. Hence, features of the object-of-interest in an image, as well as details contained in the given point cloud, can be well reconstructed.

2.1 Wavelet Frames

In this subsection, we will briefly introduce the concept of (tight) wavelet frames. Interesting readers should consult the references[4–6] for theories of (wavelet) frames and framelets, the survey paper[7] and lecture notes[8] for details on the theoretical developments and recent applications of wavelet frames.

A countable set $X \subset L_2(\mathbb{R})$ is called a tight frame of $L_2(\mathbb{R})$ if

$$f = \sum_{\psi \in X} \langle f, \psi \rangle \psi \quad \forall f \in L_2(\mathbb{R}), \tag{2.1}$$

where $\langle \cdot, \cdot \rangle$ is the inner product of $L_2(\mathbb{R})$. For given $\Psi := \{\psi_1, \ldots, \psi_r\} \subset L_2(\mathbb{R})$, the affine (or wavelet) system is defined by the collection of the dilations and the shifts of Ψ as

$$X(\Psi) := \{\psi_{\ell,j,k} : 1 \le \ell \le r;\ j, k \in \mathbb{Z}\} \quad \text{with} \quad \psi_{\ell,j,k} := 2^{j/2} \psi_\ell(2^j \cdot -k). \tag{2.2}$$

When $X(\Psi)$ forms a tight frame of $L_2(\mathbb{R})$, it is called a tight wavelet frame, and ψ_ℓ, $\ell = 1, \ldots, r$, are called the (tight) framelets.

To construct a set of framelets, usually, one starts from a compactly supported refinable function $\phi \in L_2(\mathbb{R})$ (a scaling function) that generates a multiresolution analysis (MRA) of $L_2(\mathbb{R})$, with a refinement mask h_0 satisfying

$$\widehat{\phi}(2\cdot) = \widehat{h}_0 \widehat{\phi}.$$

Figure 1. Piecewise linear refinable spline and framelets.

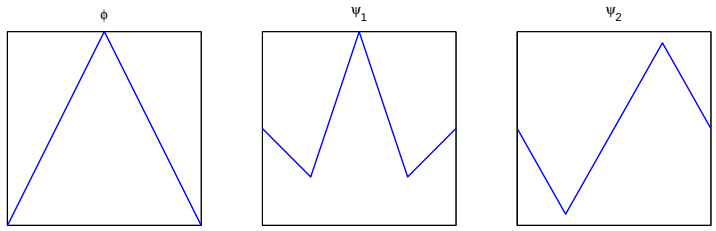

Here $\widehat{\phi}$ is the Fourier transform of ϕ, and $\widehat{h}_0$ is the Fourier series of h_0. For a given compactly supported refinable function, the construction of a tight framelet system is to find a finite set Ψ that can be represented in the Fourier domain as

$$\widehat{\psi}_\ell(2\cdot) = \widehat{h}_\ell \widehat{\phi}$$

for some 2π-periodic $\widehat{h}_\ell$. The unitary extension principle (UEP)[5] shows that the system $X(\Psi)$ in (2.2) generated by Ψ forms a tight frame in $L_2(\mathbb{R})$ provided that the masks $\widehat{h}_\ell$ for $\ell = 0, 1, \ldots, r$ satisfy

$$\sum_{\ell=0}^{r} |\widehat{h}_\ell(\xi)|^2 = 1 \quad \text{and} \quad \sum_{\ell=0}^{r} \widehat{h}_\ell(\xi)\overline{\widehat{h}_\ell(\xi+\pi)} = 0 \tag{2.3}$$

for almost all ξ in $\mathbb{R}$. While h_0 corresponds to a lowpass filter, $\{h_\ell; \ell = 1, 2, \ldots, r\}$ must correspond to highpass filters by the UEP (2.3). The sequences of Fourier coefficients of $\{h_\ell; \ell = 1, 2, \ldots, r\}$ are called *framelet masks*. In our implementation, we adopt the piecewise linear B-spline framelets.[5] The refinement mask is $\widehat{h}_0(\xi) = \cos^2(\frac{\xi}{2})$, whose corresponding lowpass filter is $h_0 = \frac{1}{4}[1, 2, 1]$. The two framelet masks are $\widehat{h}_1 = -\frac{\sqrt{2}i}{2}\sin(\xi)$ and $\widehat{h}_2 = \sin^2(\frac{\xi}{2})$, whose corresponding highpass filters are

$$h_1 = \frac{\sqrt{2}}{4}[1, 0, -1], \quad h_2 = \frac{1}{4}[-1, 2, -1].$$

The associated refinable function and framelets are given in Figure 1. With a one-dimensional framelet system for $L_2(\mathbb{R})$, the s-dimensional framelet system for $L_2(\mathbb{R}^s)$ can be easily constructed by tensor products of one-dimensional framelets.[4,8]

In the discrete setting, a discrete image u is an s-dimensional array. We use W to denote fast tensor product framelet decomposition and use $W^\top$ to denote the fast reconstruction.[8] Then by the UEP, we have $W^\top W = I$, i.e. $u = W^\top W u$ for any image u. We will further denote an L-level framelet decomposition of u as

$$Wu = \{W_{l,\boldsymbol{j}} u : 0 \le l \le L-1, \boldsymbol{j} \in I\},$$

where I denotes the index set of all framelet bands.

2.2 Wavelet Frame Based Approaches and Fast Algorithms

2.2.1 Wavelet Frame Based Model

We now present a wavelet frame based model for both image segmentation and surface reconstruction problems. The model is given as follows:

$$\min_{u \in V, \boldsymbol{c} \in \mathbb{R}^m} \|\boldsymbol{\lambda} \cdot Wu\|_1 + H(u, \boldsymbol{c}, f), \tag{2.4}$$

and

$$\|\boldsymbol{\lambda} \cdot Wu\|_1 := \left\| \sum_{l=0}^{L-1} \left(\sum_{\boldsymbol{j} \in I} \lambda_{l,\boldsymbol{j}} |W_{l,\boldsymbol{j}} u|^2 \right)^{\frac{1}{2}} \right\|_1, \tag{2.5}$$

where V is some convex set, $W_{l,\boldsymbol{j}}$ is the part of framelet decomposition corresponding to the lth level and $\boldsymbol{j}$th band; and $\lambda_{l,\boldsymbol{j}}$ is some preassigned and spatially variant parameter. If $u^\star$ is the minimizer of (2.4), then for some fixed scalar $\gamma \in [0,1]$ we have $\Omega_1 = \{x \in \Omega : u^\star(x) \leq \gamma\}$ and $\Omega_2 = \Omega_1^c$ for image segmentation; and $\mathcal{S} = \{x \in \Omega : u^\star(x) = \gamma\}$ for surface reconstruction.

REMARK 1. *The ℓ_1-norm given by* (2.5) *is known as the isotropic ℓ_1-norm of wavelet frame coefficients.*[1] *The anisotropic counterpart, defined as follows, is the standard ℓ_1-norm commonly used in the literature:*

$$\|\boldsymbol{\lambda} \cdot Wu\|_1 := \left\| \sum_{l,\boldsymbol{j}} \lambda_{l,\boldsymbol{j}} \left| W_{l,\boldsymbol{j}} u \right| \right\|_1 .$$

It was found that the isotropic ℓ_1-norm was superior than the anisotropic ℓ_1-norm in terms of both quality of the image restoration and efficiency of the corresponding numerical algorithm.[1] *This is the reason why we focus on the isotropic ℓ_1-norm in this paper.*

2.2.2 Fast Optimization Algorithm

To solve the frame based model (2.4), we apply the split Bregman algorithm[36,86] together with a coordinate descend strategy[87,88] that handles optimization with multiple variables. The split Bregman algorithm was first proposed by Goldstein and Osher[86] and was shown to be powerful in solving various variational models, e.g. ROF and nonlocal variational models.[86,89] Convergence analysis of the split Bregman algorithm was later provided for wavelet frame based image restoration model.[36] It was recently realized that the split Bregman algorithm is equivalent to the alternating direction method of multipliers (ADMM)[90–92] applied to the augmented Lagrangian of the underlying optimization problem.[93–95]

Now, we briefly describe the idea of the derivation of the algorithm based on the augmented Lagrangian method.[93–95] Introducing a new variable d in (2.4) and setting $d = Wu$, then the model (2.4) can be rewritten equivalently as

$$\min_{u \in V, \boldsymbol{c} \in \mathbb{R}^m} \|\boldsymbol{\lambda} \cdot d\|_1 + H(u, \boldsymbol{c}, f) \quad \text{s.t. } d = Wu. \tag{2.6}$$

Then the augmented Lagrangian for (2.6) can be written as

$$\mathcal{L}(u, d, \boldsymbol{c}, v) = \|\boldsymbol{\lambda} \cdot d\|_1 + H(u, \boldsymbol{c}, f) + \langle v, Wu - d \rangle + \frac{\mu}{2} \|Wu - d\|_2^2,$$

for some $\mu > 0$. Then the augmented Lagrangian method can be described as an iteration of the following two steps:

$$\begin{cases} (u^{k+1}, d^{k+1}, \boldsymbol{c}^{k+1}) = \arg \min_{u \in V, d, \boldsymbol{c}} \mathcal{L}(u, d, \boldsymbol{c}, v^k) \\ v^{k+1} = v^k + \delta(Wu^{k+1} - d^{k+1}), \end{cases} \tag{2.7}$$

for some $\delta > 0$. If we solve the first optimization problem of (2.7) in an alternative fashion (also known as the coordinate descend method[87,88]) and choose $\delta = \mu$, then after some simply manipulations of the augmented Lagrangian,[8,96,97] we obtain the fast algorithm for the wavelet frame based model (2.4) which is summarized in Algorithm 1. Note that the operator $\mathcal{T}_\lambda(\cdot)$ in (2.8) is the isotropic shrinkage operator[1,98] (corresponding to the isotropic ℓ_1-norm we are using in (2.5)), and the second identity of (2.8) is a well-known result that can be easily verified.[19]

2.2.3 Particular Models and Algorithms

Model (2.4) and the Algorithm 1 take different forms for image segmentation and surface reconstruction problems. As an example, we present the following wavelet frame based models and their corresponding algorithms, which are also the ones we use in our simulations.

Algorithm 1 Fast Algorithm for Model (2.4)

Given an input f, fix the space V, and select the parameters $\boldsymbol{\lambda}$ and $\mu > 0$. Initialize the algorithm by choosing $u^0 = 0$, $d^0 = 0$, $\boldsymbol{c}^0 = \boldsymbol{c}_0$, $v^0 = 0$, and $k = 0$.

while stopping criteria are not met **do**

1. Update u:

$$u^{k+\frac{1}{2}} = \arg\min_u H(u, \boldsymbol{c}^k, f) + \frac{\mu}{2}\|Wu - d^k + v^k\|_2^2.$$

$$u^{k+1} = \mathcal{P}_V(u^{k+\frac{1}{2}}),$$

where $\mathcal{P}_V$ is a projection operator onto V.

2. Update d:

$$\begin{aligned} d^{k+1} &= \arg\min_d \|\boldsymbol{\lambda} \cdot d\|_1 + \frac{\mu}{2}\|d - (Wu^{k+1} + v^k)\|_2^2 \\ &= \mathcal{T}_{\boldsymbol{\lambda}/\mu}(Wu^{k+1} + v^k). \end{aligned} \tag{2.8}$$

3. Update $\boldsymbol{c}$:

$$\boldsymbol{c}^{k+1} = \arg\min_{\boldsymbol{c}} H(u^{k+1}, \boldsymbol{c}, f).$$

4. Update v:

$$v^{k+1} = v^k + Wu^{k+1} - d^{k+1}.$$

5. $k = k + 1$.

end while

Image Segmentation:

Given an observed image f, consider the following wavelet frame based image segmentation model[2]

$$\min_{0 \le u \le 1, (c_1, c_2) \in \mathbb{R}^2} \|\boldsymbol{\lambda} \cdot Wu\|_1 + \langle (c_1 - f)^2 - (c_2 - f)^2, u \rangle, \tag{2.9}$$

and, for all $0 \le l \le L$ and $\boldsymbol{j} \in I$,

$$\lambda_{l,\boldsymbol{j}} = \frac{\alpha}{1 + \sigma \sum_{l,\boldsymbol{j}} |W_{l,\boldsymbol{j}} f|^2}.$$

The fast algorithm for (2.9) can be easily derived from Algorithm 1. We summarize it in Algorithm 2. Note that the operation $M(f, \Omega)$ in step 3 outputs the mean value of f within the domain Ω.

Surface Reconstruction Model:

Given a set of scattered points $\boldsymbol{X} = \{x_1, x_2, \ldots, x_n\} \subset \Omega \subset \mathbb{R}^3$, find the distance function $\varphi(x)$ defined as

$$\varphi(x) := \inf_{y \in \boldsymbol{X}} \|x - y\|_2, \quad x \in \Omega, \tag{2.10}$$

which can be obtained by solving the Eikonal's equation.[99,100] The distance function was first used by Zhao et al.[72] for surface reconstruction problems, and was used and analyzed by various later work[75,101,102] as well.

Then, we consider the following wavelet frame based surface reconstruction model[3]

$$\min_{0 \le u \le 1} \|\boldsymbol{\lambda} \cdot Wu\|_1 + \langle 2f - 1, u \rangle, \tag{2.11}$$

and, for all $0 \le l \le L$ and $\boldsymbol{j} \in I$,

$$\lambda_{l,\boldsymbol{j}} = \alpha\varphi(x),$$

with some scalar $\alpha > 0$. Here, we take f as a characteristic function, i.e. $f = \chi_\Lambda$, where $\partial\Lambda$ is an initial approximation to the surface $\mathcal{S}$ from which the given data set $\boldsymbol{X}$ is sampled. In other words, the role of f in (2.11) is to provide an initial guess to the surface $\mathcal{S}$ that we want to reconstruct. Similar to image segmentation,

Algorithm 2 Fast Algorithm for Image Segmentation[2]

Given an input image f, select the parameters (α, σ) in $\boldsymbol{\lambda}$, and pick $\mu > 0$ and $\gamma \in [0,1]$. Initialize the algorithm by choosing $u^0 = 0$, $d^0 = 0$, $c_1^0 = 1$, $c_2^0 = 0$, $v^0 = 0$, and $k = 0$.

while stopping criteria are not met **do**

1. Update u:

$$u^{k+\frac{1}{2}} = W^\top(d^k - v^k) - \frac{1}{\mu}\left((c_1^k - f)^2 - (c_2^k - f)^2\right).$$

$$u^{k+1} = \max\{\min\{u^{k+\frac{1}{2}}, 1\}, 0\}.$$

2. Update d:

$$d^{k+1} = \mathcal{T}_{\boldsymbol{\lambda}/\mu}(Wu^{k+1} + v^k).$$

3. Update $\boldsymbol{c} = (c_1, c_2)$:

$$c_1^{k+1} = M(f, \Omega^{k+1}), \quad c_2^{k+1} = M(f, (\Omega^{k+1})^c), \quad \Omega^{k+1} = \{u^{k+1} > \gamma\}.$$

4. Update v:

$$v^{k+1} = v^k + Wu^{k+1} - d^{k+1}.$$

5. $k = k + 1$.

end while

Output:

$$\Omega_1 = \{x \in \Omega : u^{\bar{k}} \leq \gamma\} \quad \text{and} \quad \Omega_2 = \Omega_1^c,$$

with $\bar{k}$ the stopping iteration.

Algorithm 3 Fast Algorithm for Surface Reconstruction[2]

Given an input $f = \chi_{\Omega^0}$ with $\partial\Omega^0$ an initial approximation to the surface to be reconstructed, compute the distance function φ by solving the Eikonal's equation and pick the parameters α, $\mu > 0$ and $\gamma \in [0,1]$. Initialize the algorithm by choosing $u^0 = 0$, $d^0 = 0$, $v^0 = 0$, and $k = 0$.

while stopping criteria are not met **do**

1. Update u:

$$u^{k+\frac{1}{2}} = W^\top(d^k - v^k) - \frac{1}{\mu}(2f - 1).$$

$$u^{k+1} = \max\{\min\{u^{k+\frac{1}{2}}, 1\}, 0\}.$$

2. Update d:

$$d^{k+1} = \mathcal{T}_{\boldsymbol{\lambda}/\mu}(Wu^{k+1} + v^k).$$

4. Update v:

$$v^{k+1} = v^k + Wu^{k+1} - d^{k+1}.$$

5. $k = k + 1$.

end while

Output:

$$\bar{\Omega} = \{x \in \Omega : u^{\bar{k}} \leq \gamma\},$$

with $\bar{k}$ the stopping iteration and $\partial\bar{\Omega}$ the reconstructed surface.

the fast algorithm for the surface reconstruction model (2.11) can be derived from Algorithm 1. We summarize it in Algorithm 3.

REMARK 2.

1. *Under certain conditions, the wavelet frame based model* (2.4) *can be shown to be a certain discretization of the following variational model*[1]

$$\min_{u\in V, \boldsymbol{c}\in\mathbb{R}^m} \|\boldsymbol{\nu}\cdot\boldsymbol{D}(u)\|_1 + H(u,\boldsymbol{c},f), \tag{2.12}$$

where $\boldsymbol{D} := \{D_{\boldsymbol{j}} : 1 \le |\boldsymbol{j}| \le s\}$ *is a vector of differential operators of order* s *and*

$$\|\boldsymbol{\nu}\cdot\boldsymbol{D}(u)\|_1 := \left\| \left(\sum_{1\le|\boldsymbol{j}|\le s} \nu_{\boldsymbol{j}} |D_{\boldsymbol{j}} u|^2 \right)^{\frac{1}{2}} \right\|_1 .$$

2. *The variational model* (2.12) *includes some of the well-known segmentation and surface reconstruction models in the literature. For example, it includes the partially convexified two-phases segmentation model*[50,51] *of the Chan-Vese model*[46,47] *as a special case:*

$$\min_{0\le u\le 1, (c_1,c_2)\in\mathbb{R}^2} \|\boldsymbol{\nu}\cdot\nabla u\|_1 + \langle (c_1-f)^2 - (c_2-f)^2, u\rangle. \tag{2.13}$$

Also, when

$$V = L_2(\Omega), \quad \boldsymbol{D} = \nabla \quad \text{and} \quad H(u,\boldsymbol{c},f) = \frac{1}{2h}\|u-f\|_2^2,$$

the variational model (2.12) *becomes the surface reconstruction model used (iteratively) by Goldstein, Bresson and Osher.*[74] *In addition, the variational model*

$$\min_{0\le u\le 1} \|\boldsymbol{\nu}\cdot\nabla u\|_1 + \langle 2f-1, u\rangle \tag{2.14}$$

was used by Ye et al.[75] *as the first step of their entire surface reconstruction procedure.*

3. *The discretization provided by wavelet frames is also a good discretization, and is generally superior than variational models discretized in a standard manner.*[27,36–38] *The wavelet frame based approaches have a built-in adaptive mechanism via the multiresolution analysis that provides a natural tool for this purpose. To illustrate the benefit of using the wavelet frame based model* (2.4) *for image segmentation and surface reconstruction, we present some 2D comparisons (Figure 2) of the variational models* (2.13) *and* (2.14) *with the wavelet frame based models* (2.9) *and* (2.11). *Note that all parameters were properly chosen for optimal segmentation and surface reconstruction results.*

3. SIMULATIONS

In this section, we present some numerical results for image segmentation and surface reconstruction. We refer the interested readers to the original work for more examples (such as 3D medical image segmentation).[2,3]

3.1 Image Segmentation

We apply Algorithm 2 to several test images that we obtained online. Large Gaussian white noise is added to these images beforehand. We fix our choices of parameters $\alpha = 0.02$, $\sigma = \frac{50}{255^2}$, $\mu = 5$ and $\gamma = 0.5$ for all the test images. The wavelet frame system is chosen to be the piecewise linear tight wavelet frame system constructed from B-spline of order 1^5 (see the example given in Section 2.1), and the level of decomposition is chosen to be 1, i.e. $L = 1$. We adopt the following stopping criterium

$$\frac{\|Wu^k - \alpha^k\|_2}{\|f\|_2} < 10^{-4}.$$

The test images and the segmentation results are shown in Figure 3.

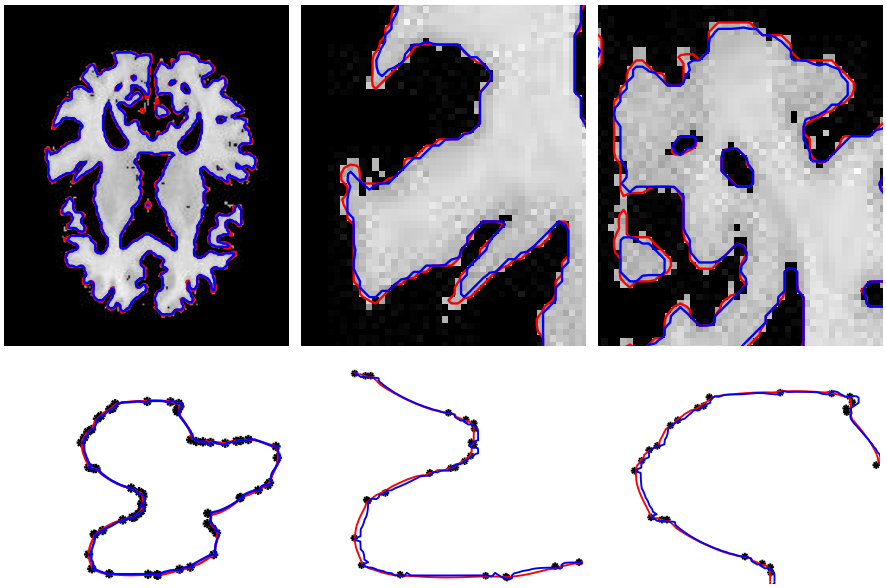

Figure 2. Comparisons in 2D for image segmentation (first row) and surface reconstruction (second row). The blue curves are the results of variational models (2.13) and (2.14); and the red curves are the results of wavelet frame based models (2.9) and (2.11). Images in the second and third columns are zoom-in views of the first column.

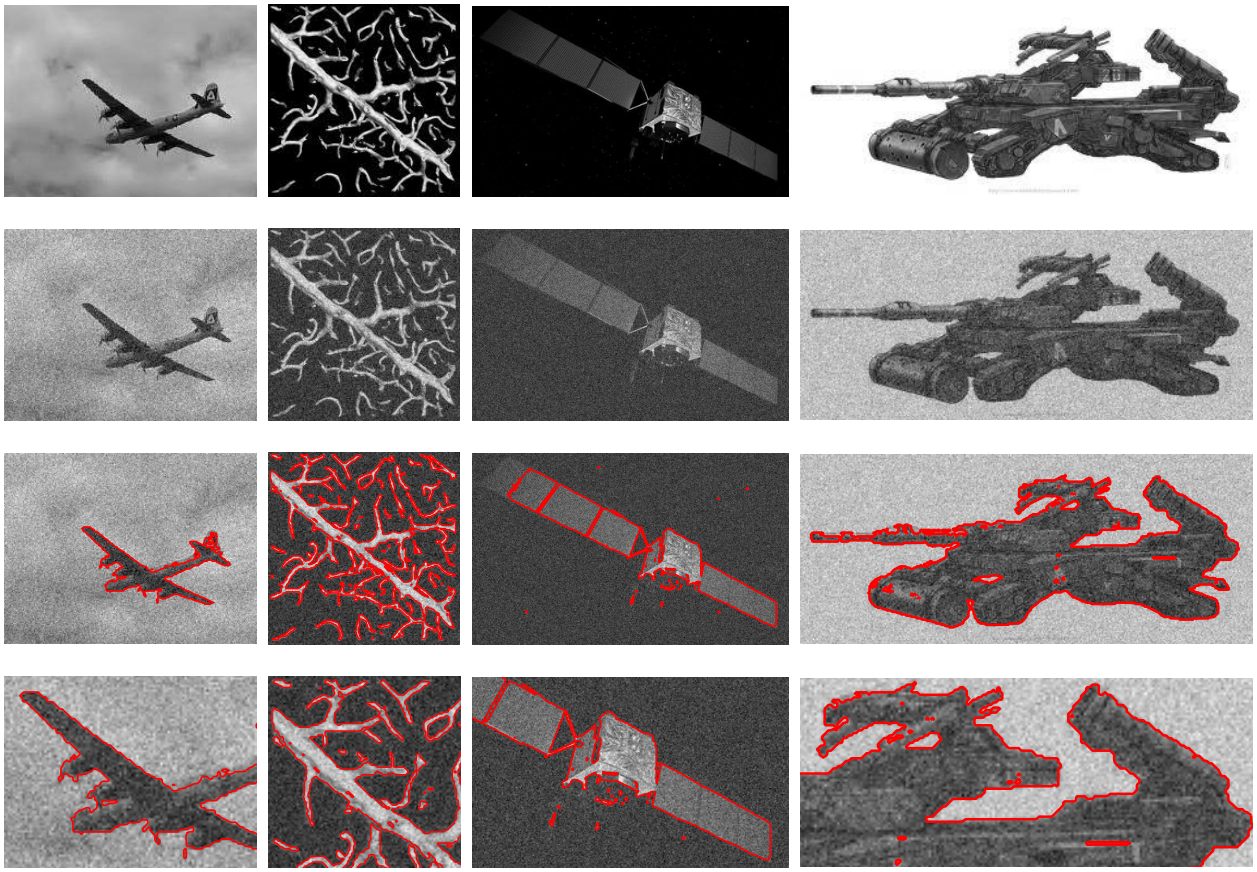

Figure 3. Image segmentation: the first row presents the original images; the second row presents the corresponding noisy images; the third row presents the segmentation results with $\partial\Omega_1$ label in red; the fourth row presents the zoom-in views corresponding to the images in the third row.

3.2 Surface Reconstruction

We apply Algorithm 3 to reconstruct surfaces from three point sets: "Asian Dragon", "Thai Statue" and "Lucy". All the point data is obtained from the Stanford 3D Scanning Repository (URL: www-graphics .stanford .edu /data /3Dscanrep) created by the Stanford Computer Graphics Laboratory. We fix the parameters $\alpha = 500$, $\mu = 0.04$ and $\gamma = 0.5$ for all the data, and adopt the following stopping criterium

$$\frac{\|u^{k+1} - u^k\|_2}{\|u^k\|_2} < 5 \times 10^{-4}.$$

Same as image segmentation, the wavelet frame system is chosen to be the piecewise linear tight wavelet frame system constructed from B-spline of order 1,[5] and the level of decomposition is chosen to be 1. The grid sizes of the computation domain Ω for the three point data are $271 \times 160 \times 187$ ("Asian Dragon"), $201 \times 324 \times 177$ ("Thai Statue") and $221 \times 136 \times 364$ ("Lucy").

To get better initialization f, we adopt the idea proposed by Ye et al.[75] Given a point set $\boldsymbol{X}$ and its corresponding distant function $\varphi(x)$, we compute f by solving the following Eikonal's equation using fast sweeping method[100]

$$|\nabla f| = \frac{1}{\varphi^2 + \varepsilon}$$

where ε is some properly chosen parameter. We shall skip the details here, but interested reader should consult Ye et al.[75] and Zhao[100] for details.

The reconstructed surfaces are presented in Figure 4, where the first row presents the initial approximation of the surface corresponding to f, and the final results are presented in the second row.

REFERENCES

[1] Cai, J., Dong, B., Osher, S., and Shen, Z., "Image restorations: total variation, wavelet frames and beyond," *preprint* (2011).

[2] Dong, B., Chien, A., and Shen, Z., "Frame based segmentation for medical images," *Communications in Mathematical Sciences* **9(2)**, 551–559 (2010).

[3] Dong, B. and Shen, Z., "Frame based surface reconstruction from unorganized points," *Journal of Computational Physics* **230**, 8247–8255 (2011).

[4] Daubechies, I., [*Ten lectures on wavelets*], vol. CBMS-NSF Lecture Notes, SIAM, nr. 61, Society for Industrial Mathematics (1992).

[5] Ron, A. and Shen, Z., "Affine Systems in $L_2(\mathbb{R}^d)$: The Analysis of the Analysis Operator," *Journal of Functional Analysis* **148**(2), 408–447 (1997).

[6] Daubechies, I., Han, B., Ron, A., and Shen, Z., "Framelets: Mra-based constructions of wavelet frames," *Applied and Computational Harmonic Analysis* **14**, 1–46 (Jan 2003).

[7] Shen, Z., "Wavelet frames and image restorations," in [*Proceedings of the International Congress of Mathematicians*], **4**, 2834–2863 (2010).

[8] Dong, B. and Shen, Z., "MRA-Based Wavelet Frames and Applications," *IAS Lecture Notes Series, Summer Program on "The Mathematics of Image Processing", Park City Mathematics Institute* (2010).

[9] Coifman, R. and Donoho, D., "Translation-invariant de-noising," *Wavelets and statistics* **103**, 125 (1995).

[10] Candes, E. and Donoho, D., "New tight frames of curvelets and optimal representations of objects with C2 singularities," *Comm. Pure Appl. Math* **56**, 219–266 (2004).

[11] Rudin, L., Osher, S., and Fatemi, E., "Nonlinear total variation based noise removal algorithms," *Phys. D* **60**, 259–268 (1992).

[12] Geman, D. and Yang, C., "Nonlinear image recovery with half-quadratic regularization," *Image Processing, IEEE Transactions on* **4**(7), 932–946 (1995).

[13] Chambolle, A. and Lions, P., "Image recovery via total variation minimization and related problems," *Numerische Mathematik* **76**(2), 167–188 (1997).

[14] Meyer, Y., [*Oscillating patterns in image processing and nonlinear evolution equations: the fifteenth Dean Jacqueline B. Lewis memorial lectures*], Amer Mathematical Society (2001).

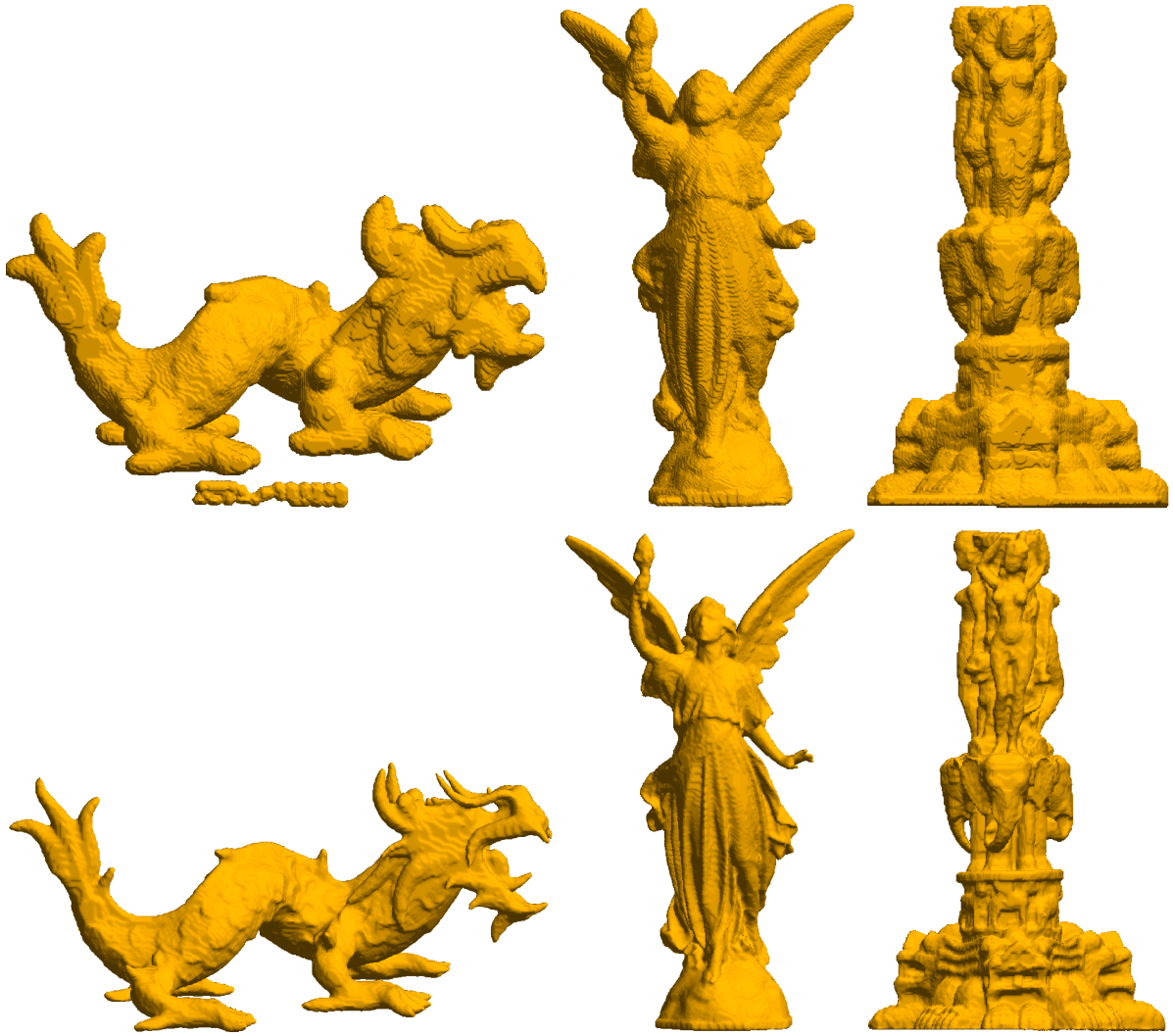

Figure 4. Surface reconstruction: the first row presents the initial approximations provided by the 0.5-level set of f; the second row presents the reconstructed surfaces.

[15] Osher, S. and Fedkiw, R., [*Level set methods and dynamic implicit surfaces*], Springer (2003).

[16] Chan, T., Esedoglu, S., Park, F., and Yip, A., "Total variation image restoration: Overview and recent developments," *Handbook of mathematical models in computer vision* , 17–31 (2006).

[17] Aubert, G. and Kornprobst, P., [*Mathematical problems in image processing: partial differential equations and the calculus of variations*], Springer (2006).

[18] Chan, T. and Shen, J., [*Image processing and analysis: variational, PDE, wavelet, and stochastic methods*], Society for Industrial Mathematics (2005).

[19] Wang, Y., Yang, J., Yin, W., and Zhang, Y., "A new alternating minimization algorithm for total variation image reconstruction," *SIAM Journal on Imaging Sciences* **1**(3), 248–272 (2008).

[20] Elad, M., Starck, J., Querre, P., and Donoho, D., "Simultaneous cartoon and texture image inpainting using morphological component analysis (MCA)," *Applied and Computational Harmonic Analysis* **19**(3), 340–358 (2005).

[21] Starck, J., Elad, M., and Donoho, D., "Image decomposition via the combination of sparse representations and a variational approach," *IEEE transactions on image processing* **14**(10), 1570–1582 (2005).

[22] Daubechies, I., Teschke, G., and Vese, L., "Iteratively solving linear inverse problems under general convex constraints," *Inverse Problems and Imaging* **1**(1), 29 (2007).

[23] Fadili, M. and Starck, J., "Sparse representations and bayesian image inpainting," *Proc. SPARS* **5** (2005).

[24] Fadili, M., Starck, J., and Murtagh, F., "Inpainting and zooming using sparse representations," *The Computer Journal* **52**(1), 64 (2009).

[25] Figueiredo, M. and Nowak, R., "An EM algorithm for wavelet-based image restoration," *IEEE Transactions on Image Processing* **12**(8), 906–916 (2003).

[26] Figueiredo, M. and Nowak, R., "A bound optimization approach to wavelet-based image deconvolution," in [*Image Processing, 2005. ICIP 2005. IEEE International Conference on*], **2**, II–782, IEEE (2005).

[27] Chan, R., Chan, T., Shen, L., and Shen, Z., "Wavelet algorithms for high-resolution image reconstruction," *SIAM Journal on Scientific Computing* **24**(4), 1408–1432 (2003).

[28] Chan, R., Riemenschneider, S., Shen, L., and Shen, Z., "Tight frame: an efficient way for high-resolution image reconstruction," *Applied and Computational Harmonic Analysis* **17**(1), 91–115 (2004).

[29] Chai, A. and Shen, Z., "Deconvolution: A wavelet frame approach," *Numerische Mathematik* **106**(4), 529–587 (2007).

[30] Cai, J., Chan, R., Shen, L., and Shen, Z., "Restoration of chopped and nodded images by framelets," *SIAM J. Sci. Comput* **30**(3), 1205–1227 (2008).

[31] Cai, J., Chan, R., Shen, L., and Shen, Z., "Convergence analysis of tight framelet approach for missing data recovery," *Advances in Computational Mathematics* **31**(1), 87–113 (2009).

[32] Cai, J., Chan, R., and Shen, Z., "A framelet-based image inpainting algorithm," *Applied and Computational Harmonic Analysis* **24**(2), 131–149 (2008).

[33] Cai, J., Chan, R., and Shen, Z., "Simultaneous cartoon and texture inpainting," *Inverse Problems and Imaging (IPI)* **4**(3), 379–395 (2010).

[34] Cai, J. and Shen, Z., "Framelet based deconvolution," *J. Comp. Math* **28**(3), 289–308 (2010).

[35] Chan, R., Shen, Z., and Xia, T., "A framelet algorithm for enhancing video stills," *Applied and Computational Harmonic Analysis* **23**(2), 153–170 (2007).

[36] Cai, J., Osher, S., and Shen, Z., "Split Bregman methods and frame based image restoration," *Multiscale Modeling and Simulation: A SIAM Interdisciplinary Journal* **8**(2), 337–369 (2009).

[37] Jia, X., Dong, B., Lou, Y., and Jiang, S., "GPU-based iterative cone-beam CT reconstruction using tight frame regularization," *Physics in Medicine and Biology* **56**, 3787–3807 (2011).

[38] Dong, B., Li, J., and Shen, Z., "X-ray CT image reconstruction via wavelet frame based regularization and Radon domain inpainting," *accepted by Journal of Scientific Computing* (2012).

[39] Zhang, Y., Dong, B., and Lu, Z., "ℓ_0 minimization of wavelet frame based image restoration," *accepted by Mathematics of Computation* (2011).

[40] Dong, B. and Zhang, Y., "An efficient algorithm for ℓ_0 minimization in wavelet frame based image restoration," *UCLA CAM Report* **11-66** (2011).

[41] Steidl, G., Weickert, J., Brox, T., Mrázek, P., and Welk, M., "On the equivalence of soft wavelet shrinkage, total variation diffusion, total variation regularization, and sides," *SIAM Journal on Numerical Analysis* **42**(2), 686–713 (2005).

[42] Mumford, D. and Shah, J., "Optimal approximations by piecewise smooth functions and associated variational problems," *Communications on pure and applied mathematics* **42**(5), 577–685 (1989).

[43] Kass, M., Witkin, A., and Terzopoulos, D., "Snakes: Active contour models," *International journal of computer vision* **1**(4), 321–331 (1988).

[44] Caselles, V., Kimmel, R., and Sapiro, G., "Geodesic active contours," *Int J Comput Vision* **22**, 61–79 (Jan 1997).

[45] Malladi, R., Sethian, J., and Vemuri, B., "Shape modeling with front propagation: A level set approach," *Pattern Analysis and Machine Intelligence, IEEE Transactions on* **17**(2), 158–175 (1995).

[46] Chan, F. and Vese, L., "An active contour model without edges," *Scale-Space Theories in Computer Vision* **1682**, 141–151 (1999).

[47] Chan, F. and Vese, L., "Active contours without edges," *IEEE Transactions on image processing* **10**(2), 266–277 (2001).

[48] Kimmel, R., "Fast edge integration," *Geometric Level Set Methods in Imaging, Vision, and Graphics* , 59–77 (2003).

[49] Kimmel, R. and Bruckstein, A., "Regularized laplacian zero crossings as optimal edge integrators," *International Journal of Computer Vision* **53**(3), 225–243 (2003).

[50] Chan, T., Esedoglu, S., and Nikolova, M., "Algorithms for finding global minimizers of image segmentation and denoising models," *SIAM Journal on Applied Mathematics* **66**(5), 1632–1648 (2006).

[51] Bresson, X., Esedoglu, S., Vandergheynst, P., Thiran, J., and Osher, S., "Fast global minimization of the active contour/snake model," *Journal of Mathematical Imaging and Vision* **28**(2), 151–167 (2007).

[52] Brown, E., Chan, T., and Bresson, X., "Completely convex formulation of the chan-vese image segmentation model," *International Journal of Computer Vision* , 1–19 (2011).

[53] Bae, E. and Tai, X., "Efficient global minimization methods for image segmentation models with four regions," *UCLA CAM Report* **11-82** (2011).

[54] Chen, Y., Tagare, H., Thiruvenkadam, S., Huang, F., Wilson, D., Gopinath, K., Briggs, R., and Geiser, E., "Using prior shapes in geometric active contours in a variational framework," *International Journal of Computer Vision* **50**(3), 315–328 (2002).

[55] Park, F., "Image segmentation using clique based shape prior and the mumford shah functional," *UCLA CAM Report* **10-87** (2010).

[56] Ye, J., Wittman, T., Bresson, X., and Osher, S., "Segmentation for hyperspectral images with priors," *Advances in Visual Computing* , 97–106 (2010).

[57] Unser, M., "Texture classification and segmentation using wavelet frames," *IEEE Transactions on image processing* **4**(11), 1549–1560 (1995).

[58] Arivazhagan, S. and Ganesan, L., "Texture segmentation using wavelet transform," *Pattern Recognition Letters* **24**(16), 3197–3203 (2003).

[59] McInerney, T. and Terzopoulos, D., "Deformable models in medical image analysis: a survey," *Medical image analysis* **1**(2), 91–108 (1996).

[60] Goldenberg, R., Kimmel, R., Rivlin, E., and Rudzsky, M., "Cortex segmentation: A fast variational geometric approach," *Medical Imaging, IEEE Transactions on* **21**(12), 1544–1551 (2002).

[61] Xue, H., Srinivasan, L., Jiang, S., Rutherford, M., Edwards, A., Rueckert, D., and Hajnal, J., "Automatic segmentation and reconstruction of the cortex from neonatal mri," *Neuroimage* **38**(3), 461–477 (2007).

[62] Tu, Z., Narr, K., Dollar, P., Dinov, I., Thompson, P., and Toga, A., "Brain anatomical structure segmentation by hybrid discriminative/generative models," *IEEE Transactions on Medical Imaging* **27**(4), 495–508 (2008).

[63] Yang, J., Staib, L., and Duncan, J., "Neighbor-constrained segmentation with 3d deformable models," in [*Information Processing in Medical Imaging*], 198–209, Springer (2003).

[64] Pizer, S., Fletcher, P., Joshi, S., Thall, A., Chen, J., Fridman, Y., Fritsch, D., Gash, A., Glotzer, J., Jiroutek, M., et al., "Deformable m-reps for 3d medical image segmentation," *International Journal of Computer Vision* **55**(2), 85–106 (2003).

[65] Tsai, A., Yezzi, A., Wells, W., Tempany, C., Tucker, D., Fan, A., Grimson, W., and Willsky, A., "A shape-based approach to the segmentation of medical imagery using level sets," *IEEE Transactions on Medical Imaging* **22**(2), 137–154 (2003).

[66] Flasque, N., Desvignes, M., Constans, J., and Revenu, M., "Acquisition, segmentation and tracking of the cerebral vascular tree on 3D magnetic resonance angiography images," *Medical Image Analysis* **5**(3), 173–183 (2001).

[67] Nain, D., Yezzi, A., and Turk, G., "Vessel segmentation using a shape driven flow," in [*Medical image computing and computer-assisted intervention - MICCAI 2004*], **3216**, 51, Springer (2004).

[68] Kirbas, C. and Quek, F., "A review of vessel extraction techniques and algorithms," *ACM Computing Surveys* **36**(2), 81–121 (2004).

[69] Hoppe, H., DeRose, T., Duchamp, T., McDonald, J., and Stuetzle, W., "Surface reconstruction from unorganized points," in [*ACM SIGGRAPH Computer Graphics*], **26**, 71–78, ACM (1992).

[70] Turk, G. and O'Brien, J., "Shape transformation using variational implicit functions," in [*ACM SIGGRAPH 2005 Courses*], 13–es, ACM (2005).

[71] Carr, J., Beatson, R., Cherrie, J., Mitchell, T., Fright, W., McCallum, B., and Evans, T., "Reconstruction and representation of 3D objects with radial basis functions," in [*Proceedings of the 28th annual conference on Computer graphics and interactive techniques*], 67–76, ACM (2001).

[72] Zhao, H., Osher, S., Merriman, B., and Kang, M., "Implicit and non-parametric shape reconstruction from unorganized points using variational level set method," *Computer Vision and Image Understanding* **80**(3), 295–319 (2000).

[73] Ye, J., Yanovsky, I., Dong, B., Gandlin, R., Brandt, A., and Osher, S., "Multigrid narrow band surface reconstruction via level set functions," *UCLA CAM Reports* **09–98** (2009).

[74] Goldstein, T., Bresson, X., and Osher, S., "Geometric applications of the split bregman method: Segmentation and surface reconstruction," *Journal of Scientific Computing* **45**(1), 272–293 (2010).

[75] Ye, J., Bresson, X., Goldstein, T., and Osher, S., "A Fast Variational Method for Surface Reconstruction from Sets of Scattered Points," *CAM Report* **10-01** (2010).

[76] Ohtake, Y., Belyaev, A., Alexa, M., Turk, G., and Seidel, H., "Multi-level partition of unity implicits," in [*ACM SIGGRAPH 2005 Courses*], 173, ACM (2005).

[77] Kolluri, R., "Provably good moving least squares," *ACM Transactions on Algorithms (TALG)* **4**(2), 1–25 (2008).

[78] Levin, D., "Mesh-independent surface interpolation," *Geometric Modeling for Scientific Visualization* **3** (2003).

[79] Alexa, M., Behr, J., Cohen-Or, D., Fleishman, S., Levin, D., and Silva, C., "Computing and rendering point set surfaces," *IEEE Transactions on Visualization and Computer Graphics* **9**, 3–15 (2003).

[80] Amenta, N., Bern, M., and Kamvysselis, M., "A new Voronoi-based surface reconstruction algorithm," in [*Proceedings of the 25th annual conference on Computer graphics and interactive techniques*], 415–421, ACM (1998).

[81] Boissonnat, J. and Cazals, F., "Smooth surface reconstruction via natural neighbour interpolation of distance functions," in [*Proceedings of the sixteenth annual symposium on Computational geometry*], 223–232, ACM (2000).

[82] Amenta, N., Choi, S., and Kolluri, R., "The power crust," in [*Proceedings of the sixth ACM symposium on Solid modeling and applications*], 249–266, ACM (2001).

[83] Mederos, B., Amenta, N., Velho, L., and de Figueiredo, L., "Surface reconstruction from noisy point clouds," in [*Proceedings of the third Eurographics symposium on Geometry processing*], 53, Eurographics Association (2005).

[84] Dey, T. and Goswami, S., "Provable surface reconstruction from noisy samples," *Computational Geometry* **35**(1-2), 124–141 (2006).

[85] Ji, H., Shen, Z., and Xu, Y., "Wavelet frame based scene reconstruction from range data," *Journal of Computational Physics* **229**(6), 2093–2108 (2010).

[86] Goldstein, T. and Osher, S., "The split Bregman algorithm for L1 regularized problems," *SIAM Journal on Imaging Sciences* **2**(2), 323–343 (2009).

[87] Tseng, P., "Convergence of a block coordinate descent method for nondifferentiable minimization," *Journal of optimization theory and applications* **109**(3), 475–494 (2001).

[88] Tseng, P. and Yun, S., "A coordinate gradient descent method for nonsmooth separable minimization," *Mathematical Programming* **117**(1), 387–423 (2009).

[89] Zhang, X., Burger, M., Bresson, X., and Osher, S., "Bregmanized nonlocal regularization for deconvolution and sparse reconstruction," *SIAM Journal on Imaging Sciences* **3**, 253–276 (2010).

[90] Gabay, D. and Mercier, B., "A dual algorithm for the solution of nonlinear variational problems via finite element approximation," *Computers & Mathematics with Applications* **2**(1), 17–40 (1976).

[91] Bertsekas, D. and Tsitsiklis, J., [*Parallel and distributed computation: numerical methods*], Prentice-Hall, Inc. (1989).

[92] Eckstein, J. and Bertsekas, D., "On the douglasrachford splitting method and the proximal point algorithm for maximal monotone operators," *Mathematical Programming* **55**(1), 293–318 (1992).

[93] Hestenes, M., "Multiplier and gradient methods," *Journal of optimization theory and applications* **4**(5), 303–320 (1969).

[94] Powell, M., "A method for non-linear constraints in minimization problems," *Optimization, Ed. R. Fletcher (Academic Press, New York)* , 283–298 (1969).

[95] Glowinski, R. and Le Tallec, P., [*Augmented Lagrangian and operator-splitting methods in nonlinear mechanics*], Society for Industrial Mathematics (1989).

[96] Yin, W., Osher, S., Goldfarb, D., and Darbon, J., "Bregman iterative algorithms for ℓ_1-minimization with applications to compressed sensing," *SIAM J. Imaging Sci* **1**(1), 143–168 (2008).

[97] Esser, E., "Applications of Lagrangian-based alternating direction methods and connections to split Bregman," *CAM Report* **9-31** (2009).

[98] Mrázek, P. and Weickert, J., "Rotationally invariant wavelet shrinkage," *Pattern Recognition* , 156–163 (2003).

[99] Crandall, M. and Lions, P., "Viscosity solutions of Hamilton-Jacobi equations," *Transactions of the American Mathematical Society* **277**, 1–42 (1983).

[100] Zhao, H., "A fast sweeping method for eikonal equations," *Mathematics of computation* **74**(250), 603–628 (2005).

[101] Pottmann, H. and Hofer, M., "Geometry of the squared distance function to curves and surfaces," *Visualization and mathematics III* , 221–242 (2003).

[102] Duan, Y., Yang, L., Qin, H., and Samaras, D., "Shape reconstruction from 3D and 2D data using PDE-based deformable surfaces," *Computer Vision-ECCV 2004* , 238–251, Springer (2004).